Two Photon Physics at LEP

Valery P. Andreev

Department of Physics and Astronomy,
202 Nicholson Hall,
Louisiana State University,
Baton Rouge, LA 70803, USA
e-mail: Valeri.Andreev@cern.ch

Abstract

A review of the experimental results on two photon collisions at LEP is given. Selected results on energy dependence of cross sections are presented. The total cross section for $\gamma\gamma \to hadrons$ is measured for two-photon centre-of-mass energies up to 185 GeV. The QCD predictions are tested in collisions of quasi-real photons with jet, inclusive single hadron or heavy flavour ($c\bar{c}$ and $b\bar{b}$) production, and by measurement of the total hadronic cross section in virtual $\gamma^*\gamma^*$ collisions.

Key words: two photon collisions, LEP, QCD

1 Introduction

A quasi-real photon interacts as a hadron due to quantum fluctuations into vector mesons or into quark-antiquark pairs. The $\gamma\gamma$ cross section is composed (Figure 1) by a "soft (VDM)" interaction, which can be described by hadronic phenomenology, like the Regge poles, a point like two-photon reaction, $\gamma\gamma \to q\bar{q}$, which is exactly calculable in QED (direct component) and a "hard component" (resolved or anomalous or QCD component) which implies the knowledge of the quark and gluon density in the photon. The "hard component" of two-photon interactions can be accessed in measurements of high-p_t

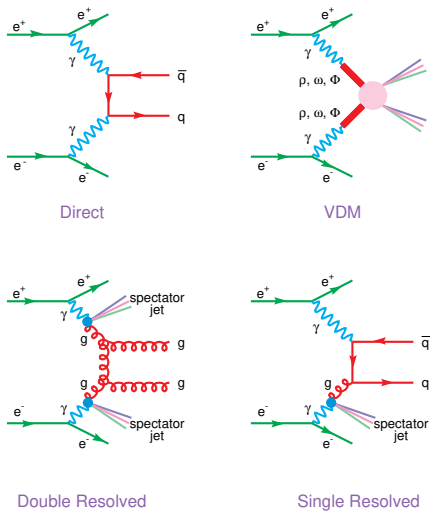

Fig. 1. Hadronic final state in two-photon collisions.

single particle and jet production, the heavy flavour production and in a scattering of highly virtual photons. A hard physical scale is given then by p_t or by c(b)-quark mass or by large virtuality Q^2 of the photon.

2 Total hadronic $\gamma\gamma$ cross section

The cross section of $\gamma\gamma \to hadrons$ process has been measured at LEP by the L3 [1,3] and the OPAL [2] for $\gamma\gamma$ centre-of-mass energies up to 185 GeV. The energy of a photon-photon collision is determined from the hadronic final state. The visible mass, W_{vis}, of the event is calculated from the four-momentum vectors of the measured particles (tracks and calorimetric clusters). The hadronic final state is not always fully contained in a detector acceptance. Unfolding procedure is applied to go from the measured W_{vis} to the true $\gamma\gamma$ centre-of-mass energy $W_{\gamma\gamma}$. From the number of events, corrected with Monte Carlo generator (PYTHIA or PHOJET) in each $W_{\gamma\gamma}$ bin, the cross section $d\sigma(e^+e^- \to e^+e^-hadrons)$ is measured, Figure 2(left). From the $d\sigma(e^+e^- \to e^+e^-hadrons)$ the total cross section of two real photons is extracted by calculating the photon flux and extrapolating the hadronic two-photon processes to zero Q^2.

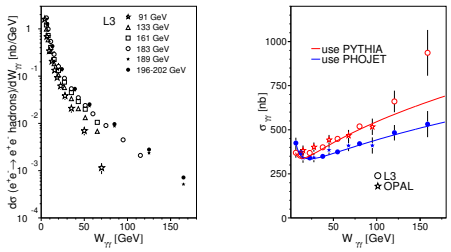

Fig. 2. Total cross section for hadron production in two-photon collisions. (left) The cross section $d\sigma(e^+e^- \to e^+e^-hadrons)/dW_{\gamma\gamma}$ measured at various LEP beam energies, 91 GeV $< \sqrt{s} <$ 202 GeV. (right) The two-photon total cross section obtained by correcting the full data sample with PYTHIA and PHOJET.

Figure 2(right) shows the $\sigma_{\gamma\gamma}$ measurements by L3 and OPAL collaborations. The difference between the open and the full dots reflects the difference on selection efficiency and unfolding corrections given by the two generators. The measurements by L3 and OPAL agree when the same generator is used in the analysis, but there is a systematic difference of order $20 \div 50$ % between the two Monte Carlo models used in analysis. This is mostly due to a different modelling of diffractive events. Discrepancy between data and predictions in a diffractive region is demonstrated by OPAL by measuring the

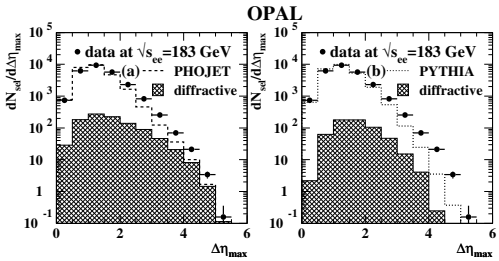

Fig. 3. Maximum rapidity gap $\Delta\eta_{max}$ distribution. The gap $\Delta\eta$ is the difference of the pseudorapidity η of any two particles, neutral or charged. Both PYTHIA and PHOJET underestimate the particle production in the diffractive region (high values of $\Delta\eta_{max}$).

maximum rapidity gap $\Delta\eta_{max}$, Figure 3. It shows that PYTHIA and PHOJET both underestimate the particle production in the diffractive region (high values of $\Delta\eta_{max}$). Finally, the cross section is given as average of the two generators, Figure 4, where a model dependence is dominating systematic error. A parametrization [4] of the cross section by the form $\sigma_{\rm tot} = A\,s^{\epsilon} + B\,s^{-\eta}$ describes well the energy behaviour of all total hadron-hadron cross sections. A fit with A, B and ϵ as free parameters ($\eta = 0.358$[5]) gives:

$\epsilon = 0.225 \pm 0.021$, L3

$\epsilon = 0.101 + 0.025/-0.019$, OPAL

The L3 ϵ value is about a factor of 2.5 higher than the universal value $\epsilon = 0.093 \pm 0.02$ [5], independent of the Monte Carlo model used to correct the data, while OPAL fit is consistent with PDG value. The L3 fit [3] shows that reggeon part (slope described by η) and Pomeron part (slope described by ϵ) of the fit are strongly correlated. Fitting only high energy part (Pomeron) the slope increases from $\epsilon = 0.116 \pm 0.016$ (the OPAL measurement range) to $\epsilon = 0.202 \pm 0.035$ for $W_{\gamma\gamma}^{min}$ from 17 GeV to 47 GeV. It means the slope is not a fundamental constant but rather illustrates the inset of QCD phenomena. The two-photon cross section at high energies can be estimated from proton-proton and photoproduction total cross sections assuming factorization for the Pomeron term: $\sigma_{\gamma\gamma} \approx \sigma^2_{\gamma p}/\sigma_{pp}$. The predictions thus obtained are consistent with the two-photon measurement, Dual Parton Model curve [8] in Figure 4(left). Several QCD inspired models [6,7,9,10] are also in a qualitative agreement with the data (Figure 4).

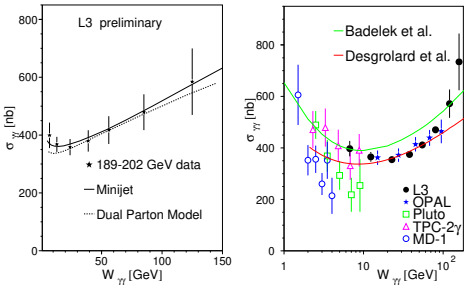

Fig. 4. Predictions for two-photon total cross section [8–10].

3 Charm and beauty production

The production of heavy quarks in two-photon collisions consists mainly of charm quarks. Because of their smaller electric charge and larger mass, the production of b-quarks is expected to be suppressed by more than two orders of magnitude relative to the production of charm quarks. The resolved photon cross section is dominated by the photon-gluon fusion diagram $\gamma g \to c\bar{c}, b\bar{b}$. At LEP energies, the direct and resolved processes are predicted to give comparable contributions to the cross section [12]. Measurements of charm production in two-photon collisions were done at LEP by ALEPH[13], DELPHI[14], L3[15,16] and OPAL[18] collaborations. Beauty production has been measured by L3[16] for the first time in gamma-gamma collisions. Preliminary result on beauty production from OPAL collaboration has been presented at PHO-

TON2000 conference.

Charm particles in the final state were identified by the reconstruction of charged D^* meson decays by ALEPH, DELPHI, L3 and OPAL. Both, charm and beauty quarks were identified by the L3 collaboration using tagging by electrons and muons from semileptonic charm and beauty decays. The total inclusive charm cross sections are plotted in Figure 5 together with previous measurements. The data are compared to the theory predictions of Ref.[12]. The dashed line corresponds to the direct process, NLO QCD calculation, while the solid line shows the QCD prediction for the sum of the direct and the resolved processes calculated to NLO accuracy. The cross section of charm production with a D^* tag is in agreement with the lepton tag measurement. In Figure 6 the DELPHI [14], L3 [25] and OPAL [18] measurements of the differential cross section $\mathrm{d}\sigma/dP_T^{D^*}$ are compared to NLO QCD calculations [24] used the massive matrix elements approach. The measurements are in agreement with each other and with QCD calculations.

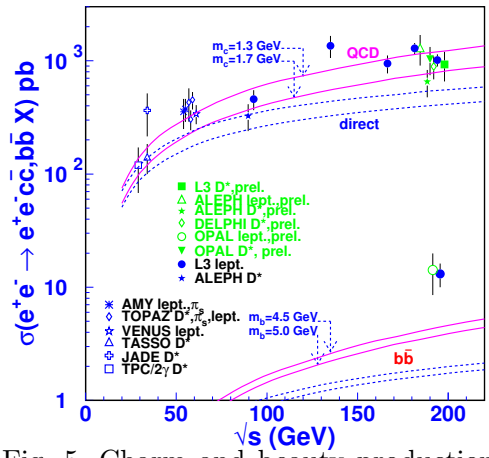

Fig. 5. Charm and beauty production in two-photon collisions.

The L3 collaboration measured the cross sections $\sigma(\mathrm{e^+e^-} \to \mathrm{e^+e^-c\bar{c}X})$ and $\sigma(\gamma\gamma \to \mathrm{c\bar{c}X})$ in the interval 5 GeV $\leq W_{\gamma\gamma} \leq$ 70 GeV[17].
Figure 7 shows the $\sigma(\gamma\gamma \to \mathrm{c\bar{c}X})$ as function of $W_{\gamma\gamma}$ at $\sqrt{s} = 189 - 202$ GeV with NLO QCD calculations [24]. In the calculations the charm mass, m_c, is fixed to 1.2 GeV, the renormalization and factorization scales are set to m_c and $2m_\mathrm{c}$, respectively, the QCD parameter Λ_5^{QCD} is set at 227.5 MeV, and the GRS-HO [26] photon parton density function is used. Using this set of input parameters, the NLO QCD predictions repro-

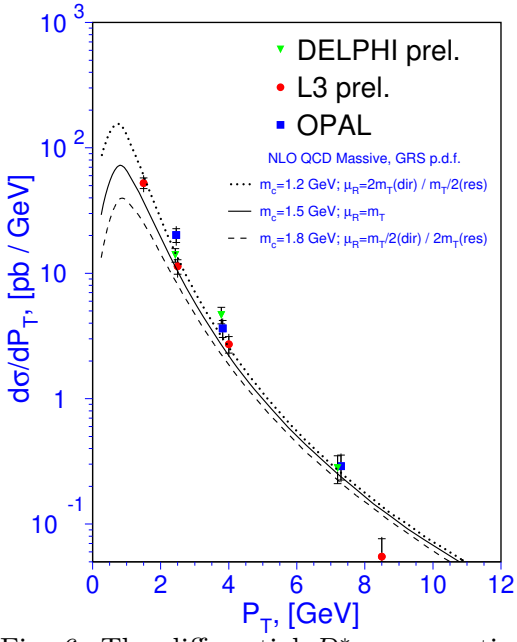

Fig. 6. The differential D^* cross section $\mathrm{d}\sigma/dP_T^{D^*}$.

duce well the energy dependence and the normalization. The calculation with $m_c = 1.5$ GeV results in about 50% lower cross section values, except the first point, where it is lower by 25%. A change in the renormalization scale from m_c to $2m_c$ decreases the QCD prediction by 10% and 30% at low and high $W_{\gamma\gamma}$ respectively. The measured charm cross section is also compared with the total cross section of hadron production in two-photon collisions [3], scaled by an arbitrary factor 1/20. A steeper rise with energy is observed as compared to hadron-hadron cross sections and to $\sigma(\gamma\gamma \to hadrons)$. The fit of the form $\sigma_{\rm tot} = A\, s^{\epsilon} + B\, s^{-\eta}$, with fixed value of $\eta = -0.358$ [5] gives for the Pomeron slope $\epsilon = 0.40 \pm 0.08$(stat).

Leptons from b semi-leptonic decays are more energetic than from charm semi-leptonic decays and non-charm two-photon processes. To select $b\bar{b}$ events L3 apply cuts on the lepton momentum and transverse momentum with respect to the closest jet defined by excluding the lepton from the jet. After all cuts are applied 137 electron and 269 muon candidates remain. The beauty purity is 42 % and 52 %, respectively. The beauty selection efficiency is 1.25 % for the electron and 2.2 % for the muon tag. The beauty production cross section in $\gamma\gamma$ collisions has been measured by L3 to be $\sigma^{ee\to eebbX} = 13.1 \pm 2.0$ (st) ± 2.4 (sys) pb. The preliminary result by OPAL using muon tag is $\sigma^{ee\to eebbX} = 14.2 \pm 2.5$ (st) ± 5.0 (sys) pb [19]. The measured b cross section lie about 4 standard deviations above QCD prediction, Figure 5. This is particularly interesting as measurements of beauty production in $p\bar{p}$ collisions by CDF [20] and DØ [21] as well as in ep collisions by H1 [22] and ZEUS [23] have been found to be a factor ∼2–3 higher than NLO QCD predictions.

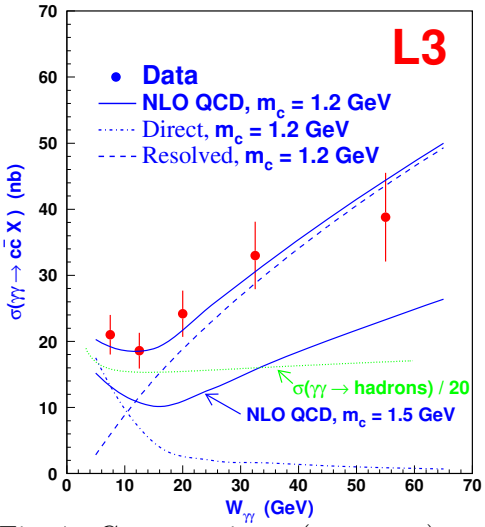

Fig. 7. Cross section $\sigma(\gamma\gamma \to c\bar{c})$ versus $W_{\gamma\gamma}$ by L3.

4 Total hadronic $\gamma^*\gamma^*$ cross section

The cross-section measurement for scattering of two virtual photons is considered as "golden" process to test the BFKL dynamics which is proposed in [27]. Double-tag events in two-photon collisions are studied by the L3 [29] and OPAL [30] collaborations at the LEP center of mass energies $\sqrt{s} \simeq 91 - 209$ GeV. The cross-section of $\gamma^*\gamma^*$ collisions is measured at an average photon virtuality up to $\langle Q^2 \rangle = 16$ GeV^2. The $\gamma^*\gamma^*$ interaction can be seen as

the interaction of two $q\bar{q}$ pairs scattering off each other via multiple gluon exchange. For the highly virtual two-photon process, with $Q_1^2 \simeq Q_2^2$, the calculation can be verified without phenomenological inputs as non-perturbative QCD contributions are expected to vanish [28]. The L3 selects [29] 137 events

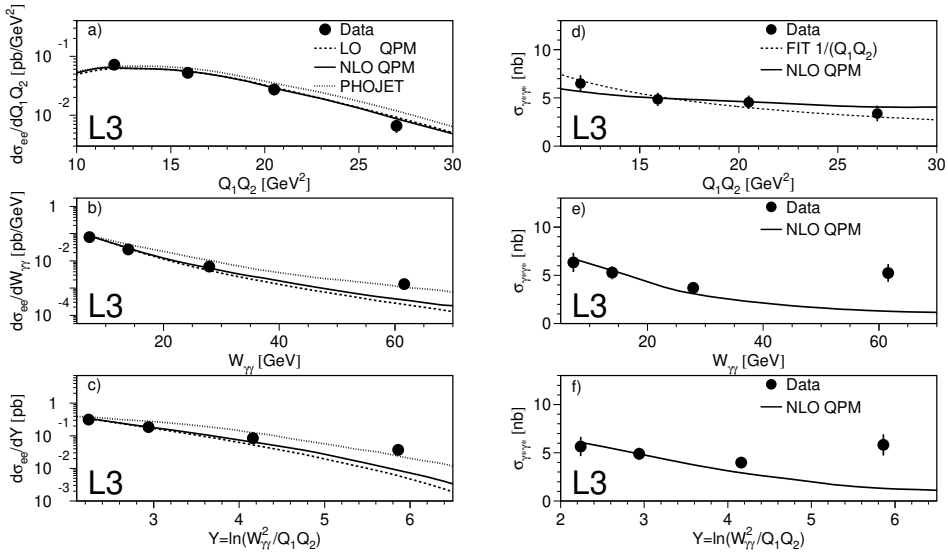

Fig. 8. The differential cross-sections of the $e^+e^- \to e^+e^- hadrons$ (a,b,c) and the cross-sections of the $\gamma^*\gamma^* \to hadrons$ processes (d,e,f) by L3.

at $\sqrt{s} \simeq 91$ GeV with $\langle Q^2 \rangle = 3.5$ GeV^2, 34 events at $\sqrt{s} \simeq 183$ GeV with $\langle Q^2 \rangle = 14$ GeV^2 and 491 events at $\sqrt{s} \simeq 189-209$ GeV with $\langle Q^2 \rangle = 16$ GeV^2. The dominant background processes are $e^+e^- \to e^+e^-\tau^+\tau^-$ and misidentified single-tagged events. The true value of $W_{\gamma\gamma}$ is calculated from the missing mass of the two scattered electrons, $W_{\rm ee}$. This avoids an unfolding procedure, which calculates $W_{\gamma\gamma}$ from the effective mass of the hadrons seen in the detector, W_{vis}. However the $W_{\rm ee}$ variable is affected by the QED radiative corrections. In the present analysis they are taken into account in the Monte Carlo generators. In Figure 8(a,b,c) the measured cross section $e^+e^- \to e^+e^-\gamma^*\gamma^* \to e^+e^- hadrons$ is plotted together with prediction for direct (QPM) process and with the prediction of QCD Monte Carlo model implemented in the PHOJET generator [8]. The cross section is plotted as

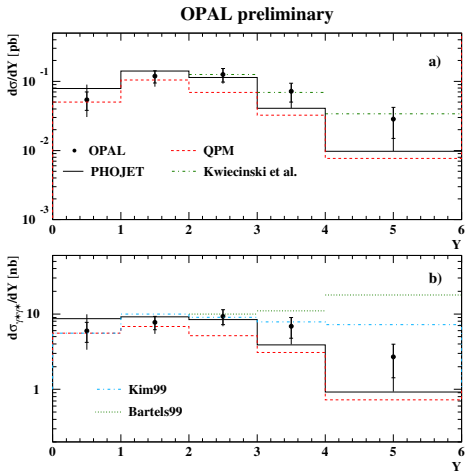

Fig. 9. The differential cross-sections of the $e^+e^- \to e^+e^- hadrons$ process (a) and the cross-sections of the $\gamma^*\gamma^* \to hadrons$ processes (b) by OPAL.

function $Q_1Q_2, W_{\gamma\gamma}$ and of variable $Y = ln(s/s_0) \simeq ln(W_{\gamma^*\gamma^*}/Q_1Q_2)$. The QPM cross section lies below the data, while QCD prediction is in a reasonable agreement with the data.

The value of the cross section at $5 < Y < 7$ exceeds the Monte Carlo prediction by about 3.5 standard deviations. This may be interpreted as a sign of resolved photon QCD processes or the onset of BFKL phenomena. The two-photon cross-section is extracted from the $e^+e^- \to e^+e^- hadrons$ cross-section, σ_{ee}, by using only the transverse photon luminosity function [31], $\sigma_{ee} = L_{TT} \cdot \sigma_{\gamma^*\gamma^*}$. The two-photon cross-section, $\sigma_{\gamma^*\gamma^*}$ is shown in Figure 8(d,e,f). Figure 9 shows preliminary measurement by the OPAL which supports the L3 observations.

5 Jet and single particle production

Di-jet production, the production of charged hadrons and K^0_S mesons in the collisions of quasi-real photons has been measured by OPAL [32]. The production of π_0 and K^0_S mesons has been measured by L3 in [33]. The inclusive two-jet cross section is shown in Figure 10(left) as a function of E_T^{jet}. The distribution is compared to a NLO QCD calculation [34]. The measured cross sections are in good agreement with NLO QCD calculations except for the first bin were the NLO calculations are not reliable.

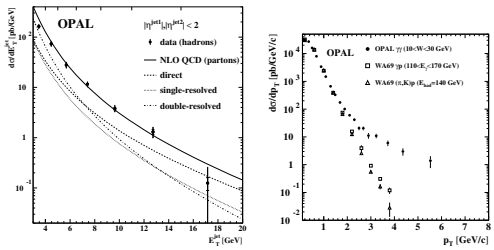

Fig. 10. (left) The inclusive two-jet cross section as a function of E_T^{jet} by OPAL compared with the NLO QCD calculations [34], (right) the charge hadron p_T distribution measured in $\gamma\gamma$ interactions is compared to the p_T distribution measured in γp and hp ($h = \pi, K$) interactions.

The inclusive two-jet cross section is dominated by the resolved processes in the low E_T^{jet} region, at high E_T^{jet} the direct process contribution is the largest. The Monte Carlo models PYTHIA and PHOJET describe the transverse energy flow around the jets reasonably well. Figure 10(right) shows the inclusive p_T distribution for the charged hadrons measured in $\gamma\gamma$ interactions by OPAL and compared to the p_T distribution measured in γp and hp ($h = \pi, K$) interactions by WA69. There is an evidence for hard photon interactions (direct process contribution) in addition to the hadronic photon interactions. A clear

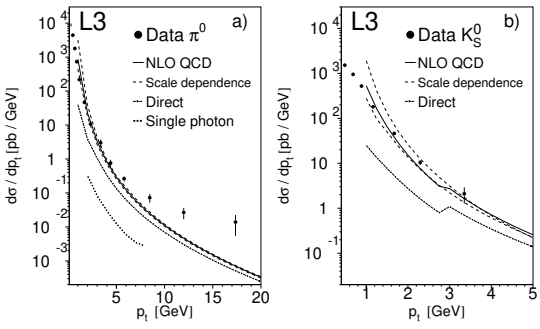

Fig. 11. The inclusive π_0 (a) and K^0_S (b) differential cross sections measured by L3, compared with NLO QCD calculations [34].

deviation is seen at large p_T from the exponential fall-off expected for purely hadronic interactions.

Figure 11 shows the inclusive p_T distribution for π_0 and K^0_S mesons measured by L3 and compared to NLO QCD calculations [34]. The transverse momentum and pseudorapidity distributions of the K^0_S mesons are well reproduced by the NLO calculations, while high p_T part of the π_0 spectrum is in excess of the prediction.

6 Outlook

Two Photon Physics studies at LEP have substantially improved (extended) the corresponding previous measurements. There are several measurements which have been performed for the first time in $\gamma\gamma$ collisions. Analysing the full LEP data sample will further contribute to this rich and important research field.

7 Acknowledgements

I would like to thank Vojtech Kundrat for the lively atmosphere of the Workshop and for the perfect organisation.

References

[1] L3 Coll., M. Acciari *et al*, Phys. Lett. **B 408** (1997) 450.

[2] OPAL Coll., K. Ackerstaff *et al*, Eur. Phys. J **C 14** (2000) 199.

[3] L3 Coll., CERN-EP/2001-012; Accepted by Phys. Lett. B.

[4] A. Donnachie and P.V. Landshoff, Phys. Lett. **B 296** (1992) 227.

[5] D.E. Groom *et al*, Review of Particle Physics, Eur. Phys. J. **C 15** (2000) 1.

[6] A. Donnachie and P.V. Landshoff, hep-ph 9806344 (1998).

[7] A. Donnachie, H.G. Dosch and M. Rueter, hep-ph 9810206 (1998).

[8] R. Engel, Z. Phys. C **66**, 203 (1995);
R. Engel and J. Ranft, Phys. Rev. D **54**, 4246 (1996).

[9] B. Badelek, J. Kwiecinski and A.M. Stasto , hep-ph 9903248 (1999).
P.Desgrolard, M. Giffon, E. Martynov and E. Predazzi, hep-ph 9811393 (1998).

[10] R.M. Godbole and G. Pancheri, hep-ph 9903331 (1999);
A. Corsetti, R.M. Godbole and G. Pancheri, Phys. Lett. **B 435** (1998) 441.

[11] L3 Coll., M. Acciari *et al.* Phys. Lett. **B 453** (1999) 83.

[12] M. Drees, M. Krämer, J. Zunft and P.M. Zerwas, Phys. Lett. B **306**, 371 (1993).

[13] ALEPH Coll., D. Buskulic *et al*, Phys. Lett. B **355**, 595 (1995); the ALEPH note 031, 2000.

[14] DELPHI Coll., M. Chapkin, V. Obraztsov and A. Sokolov, Proc. of PHOTON2000, AIP conf. proceedings, v. 571 (2000) 252;
A. Sokolov, private communication.

[15] L3 Coll., M. Acciarri *et al*, Phys. Lett. B **453**, 83 (1999); Phys. Lett. B **467**, 137 (1999).

[16] L3 Coll., M. Acciarri *et al*, Phys. Lett. B **503**, 10 (2001).

[17] L3 Coll., M. Acciarri *et al*, Phys. Lett. B **514**, 19 (2001).

[18] OPAL Coll., G. Abbiendi *et al*, Eur. Phys. J **C 16** (2000) 579.

[19] OPAL Coll., Á. Csilling, Proc. of PHOTON2000, AIP conf. proceedings, v. 571 (2000) 276.

[20] CDF Coll., F. Abe *et al*, Phys. Rev. Lett. **71**, 500,2396,2537 (1993); Phys. Rev. Lett. **75**, 1451 (1995);Phys. Rev. Lett. **79**, 572 (1997).

[21] DØColl., S. Abachi *et al*, Phys. Rev. Lett. **74**, 3548 (1995).

[22] H1 Coll. , C. Adloff *et al*, Phys. Lett. B **467**, 156 (1999).

[23] ZEUS Coll. , O. Deppe *et al*, Proc. of PHOTON99, Nucl. Phys. B. (Proc. Suppl.), **82** 206-211, 2000.

[24] S. Frixione, M. Krämer and E. Laenen, D^* *Production in Two-Photon Collisions*, Nucl. Phys. B **571**, 169 (2000); privite communication.

[25] L3 Coll., V.P. Andreev, Proc. of PHOTON2001, September 2001, Ascona, Switzerland.

[26] M. Gluck, E. Reya and I. Schienbein, Phys. Rev. D **60**, 054019 (1999).

[27] E.A. Kuraev, L.N. Lipatov and V.S. Fadin, Sov. Phys. JETP **45** (1977) 199; Ya.Ya. Balitski and L.N. Lipatov, Sov. J. Nucl. Phys. **28** (1978) 822.

[28] S.J. Brodsky *et al*, Phys. Rev. **D 56** (1997) 6957;
J. Bartels *et al*, Phys. Lett. **B 389** (1996) 742; hep-ph/9710500.

[29] L3 Coll., M. Acciari *et al.* Phys. Lett. **B 453** (1999) 333;
C.H. Lin, Proc. of PHOTON2001, September 2001, Ascona, Switzerland.

[30] OPAL Coll., M. Przybycień, Proc. of PHOTON2000, AIP conf. proceedings, v. 571 (2000) 147.

[31] V.M. Budnev *et al., Phys. Rep.* **C 15** (1975) 181. G.A. Schuler, *Comput. Phys. Commun.* **108** (1998) 279.

[32] OPAL Coll., T. Ackerstaff *et al.*, Eur. Phys. J. C **6** (1999) 253; Eur. Phys. J. C **10** (1999) 547.

[33] L3 Coll., CERN-EP/2001-065, Submitted to Phys. Lett. B.

[34] T. Kleinwort, G. Kramer, 1996 *Nucl. Phys.* B **477** 3; 1996 *Phys. Lett.* B **370** 141; M. Klasen, T. Kleinwort, G. Kramer, private communication.